[CANCER RESEARCH 59, 3761–3767, August 1, 1999]

A Senescence-like Phenotype Distinguishes Tumor Cells That Undergo Terminal Proliferation Arrest after Exposure to Anticancer Agents[1]

Bey-Dih Chang, Eugenia V. Broude, Milos Dokmanovic, Hongming Zhu, Adam Ruth, Yongzhi Xuan, Eugene S. Kandel, Ekkehart Lausch, Konstantin Christov, and Igor B. Roninson[2]

Departments of Molecular Genetics [B-D. C., E. V. B., M. D., H. Z., A. R., Y. X., E. S. K., E. L., I. B. R.] and Surgical Oncology [K. C.], University of Illinois at Chicago, Chicago, Illinois 60607-7170

ABSTRACT

Exposure of human tumor cell lines to different chemotherapeutic drugs, ionizing radiation, and differentiating agents induced morphological, enzymatic, and ploidy changes resembling replicative senescence of normal cells. Moderate doses of doxorubicin induced this senescence-like phenotype (SLP) in 11 of 14 tested cell lines derived from different types of human solid tumors, including all of the lines with wild-type p53 and half of p53-mutated cell lines. SLP induction seemed to be independent from mitotic cell death, the other major effect of drug treatment. Among cells that survived drug exposure, SLP markers distinguished those cells that became terminally growth-arrested within a small number of cell divisions from the cells that recovered and resumed proliferation. SLP induction in breast carcinoma cells treated with retinoids *in vitro* or *in vivo* was found to correlate with permanent growth inhibition under the conditions of minimal cytotoxicity, suggesting that this response may be particularly important for the antiproliferative effect of differentiating agents. The senescence-like program of terminal proliferation arrest may provide an important determinant of treatment outcome and a target for augmentation in cancer therapy.

INTRODUCTION

Exposure of tumor cells to anticancer drugs leads to growth arrest and cell death. Drug-induced cell death often shows morphological and biochemical features of apoptosis (1, 2). Another form of cell death, induced by γ-irradiation (3) and some chemotherapeutic drugs (4–6), is termed mitotic cell death or mitotic catastrophe; it is characterized by the formation of micronuclei and accumulation of karyotypic abnormalities. Although mitotic death may culminate in features of apoptosis (7), only apoptosis and not mitotic death is promoted by wild-type p53 (8) and inhibited by BCL2 (5).

Induction of cell death is generally most prominent at the highest drug doses, whereas differentiating agents and low doses of chemotherapeutic drugs have a more pronounced cytostatic effect. Cellular damage by drugs or ionizing radiation induces transient growth arrest, which depends largely on the function of $p21^{waf1/cip1}$, a p53-regulated cyclin-dependent kinase inhibitor (9, 10). On removal of the drug, most tumor cells eventually resume division and either continue to proliferate or die with features of mitotic catastrophe (7, 11). Some of the drug-treated tumor cells undergo prolonged (up to several weeks) growth arrest; such stable arrest may show features of differentiation (12) and has been described as failure to resume cell division on release from the drug (9, 11).

In normal cells, terminal proliferation arrest may result from terminal differentiation or replicative senescence. Senescence, a physiological process that limits the proliferative span of normal cells, is accompanied by morphological changes (enlarged and flattened shape and increased granularity), shortening of telomeres, and accumulation of karyotypic abnormalities (13–15). A commonly used surrogate marker of senescence in human cells is the SA-β-gal[3] active at pH 6.0; this activity was shown to correlate with senescence in aging cell cultures *in vitro* and *in vivo* (16). Treatment of normal cells with DNA-damaging drugs or γ-irradiation (17–19) or introduction of an activated *ras* oncogene (20) rapidly induces terminal proliferation arrest accompanied by morphological features of senescence and the induction of SA-β-gal. Accelerated senescence was, therefore, suggested to be a programmed protective response of the organism to potentially carcinogenic impact (21). Like other damage responses of normal cells, such as quiescence and apoptosis (2, 22), senescence-like terminal proliferation arrest involves the function of wild-type p53 (18, 20, 23).

Escape from senescence in the course of neoplastic transformation has been linked to inactivation of p53 or $p16^{INK4a}$ (20, 24) and to constitutive activation of telomerase, an enzyme complex that prevents shortening of telomeres in consequent rounds of replication (25). Immortal tumor-derived cell lines, however, were reported to express senescence markers and to undergo terminal proliferation arrest after genetic modification, such as somatic cell fusion (26) or overexpression of *p53*, *RB*, *p16*, or *p21* tumor suppressor genes (27–30). Markers of senescence were also recently reported to develop in a nasopharyngeal carcinoma cell line after exposure to cisplatin, although the association of these markers with growth-restricted cells was not examined (31). These observations suggest that tumor cells have retained at least some of the components of the senescence-like program of terminal proliferation arrest. In the present study, we show that treatment of tumor cells with different classes of anticancer agents readily induces morphological, enzymatic, and ploidy changes characteristic of senescence, and that this SLP distinguishes cells that become stably growth-arrested within a small number of cell divisions from cells that recover after drug exposure. The induction of senescence-like terminal proliferation arrest may provide an important determinant of treatment response in tumor cells.

MATERIALS AND METHODS

Cell Lines. HT1080 subline 3′SS6 was derived in our laboratory (32). HCT116 cells were a gift from Dr. B. Vogelstein (Johns Hopkins University, Baltimore, MD). Most of the other cell lines were obtained from American Type Culture Collection. Cell lines DLD1, Saos2, LNCaP, and PC3 were grown in RPMI with 10% FC2 (Hyclone) or FCS; all of the other lines were grown in DMEM with 10% serum. Cell line MCF10AneoT, a gift from Dr. F. R. Miller (Karmanos Cancer Institute, Detroit, MI), was grown as a xenograft in nude mice by transplanting 2.2×10^6 cells mixed with 0.1 ml of Matrigel into the mammary gland parenchyma of both right and left inguinal glands of nude mice.

Received 1/29/99; accepted 5/21/99.

The costs of publication of this article were defrayed in part by the payment of page charges. This article must therefore be hereby marked *advertisement* in accordance with 18 U.S.C. Section 1734 solely to indicate this fact.

[1] Supported by National Cancer Institute Grants R01CA62099 and R37CA40333 (to I. B. R.) and predoctoral fellowship DAMD17-96-1-6050 from the United States Army Medical Research and Materiel Command (to E. S. K.).

[2] To whom requests for reprints should be addressed, at Department of Molecular Genetics (M/C 669), University of Illinois at Chicago, 900 South Ashland Avenue, Chicago, IL 60607-7170. Phone: (312) 996-3486; Fax: (312) 413-8358; E-mail: roninson@uic.edu.

[3] The abbreviations used are: SA-β-gal, senescence-associated β-galactosidase; 4-HPR, 4-hydroxyphenyl retinamide; FACS, fluorescence-activated cell sorter; FISH, fluorescence *in situ* hybridization; SLP, senescence-like phenotype; tRA, all-*trans*-retinoic acid; PI, propidium iodide.

Drug Assays, Microscopic Analyses, and FISH. All of the drugs were purchased from Sigma Chemical Co.; J. L. Shepherd Model 143 irradiator was used for γ-irradiation. Growth inhibition assays were carried out by plating 4–10 × 10^4 cells/3.5-cm plate before drug exposure; cell growth was measured by methylene blue staining, as described (33). Colony formation assays were done by plating 700 cells/10-cm plate and allowing cells to form colonies for 8 days after release from the drug. MCF10AneoT xenografts were allowed to reach 4–6 mm in diameter (4–5 weeks after injection), at which point the animals were separated into two groups, five animals with 10 tumors in each group. One group was left untreated, and the other group was given 4-HPR (4 mM/kg diet) for 2 months; the growth of tumor nodules was monitored.

Attached cells and frozen tumor sections were fixed and stained for SA-β-gal activity using X-gal (5-bromo-4-chloro-3-indolyl β-D-galactoside) at pH 6.0, as described (16); the percentage of SA-β-gal+ cells was determined by bright-field microscopy after scoring 100-1000 cells for each sample. Micronuclei formation was determined after SA-β-gal staining, either by phase-contrast microscopy or after staining with H&E. [^{3}H]thymidine autoradiography was carried out as described (16).

FISH analysis of interphase nuclei was conducted by the Reproductive Genetics Institute (Chicago, IL) using mixtures of differentially labeled fluorescent probes specific for human chromosomes 18 and 21 or 13, 18, 21, X, and Y, using the hybridization conditions and scoring criteria recommended by the probe manufacturer (Vysis, Downers Grove, IL). Fluorescent cells were examined and photographed using Nicon fluorescence microscope with Photometrics Sensys camera and Quips mFISH imaging software.

FACS Assays. For DNA content analysis, 3 × 10^5 cells/6-cm plate were treated with different drugs. After treatment, floating cells were collected by centrifugation, combined with trypsinized attached cells, and analyzed by PI staining and FACS analysis using Becton Dickinson FACSort, as described (34).

For PKH2 analysis of cell division, 10^7 cells were trypsinized and labeled with PKH2 (Sigma Chemical Co.), according to the manufacturer's protocol. Cells were plated at 2 × 10^5/6-cm plate, and PKH2 fluorescence was monitored on consecutive days by FACS analysis, after PI staining to exclude dead cells. As a control for the stability of PKH2 labeling, no changes in cell fluorescence were observed in a HT1080 subline that was growth-arrested for 5 days by inducible overexpression of $p21^{waf1/cip1}$. ModFit cell cycle analysis program (Verity Software) was used to determine the percentage of cells that went through different numbers of divisions. Cell sorting was carried out using FACSvantage (Becton Dickinson) or EPICS Elite-ESP (Coulter). The sorted cells were used for SA-β-gal staining after plating 5 × 10^4 cells/3-cm plate and for clonogenic assays by plating 2000 cells/10-cm plate.

RESULTS

Moderate Doses of Cytotoxic Agents Induce Mitotic Cell Death and SLP. We have analyzed the effects of a moderate (30 nM) dose of doxorubicin, a widely used anticancer agent that acts by stabilizing "cleavable complexes" of DNA with topoisomerase II, on HT1080 human fibrosarcoma cells. This cell line carries mutant N-*ras* (35), is p16-deficient (24), and expresses wild-type Rb (36) and p53.[4] As illustrated in Fig. 1*A*, doxorubicin treatment produced a mixed cytostatic and cytotoxic effect, evidenced by pronounced growth arrest by the 2nd day of exposure and a decrease in cell number detectable from the 3rd day. The most prominent feature of cell death was the appearance of enlarged cells containing multiple completely or partially separated micronuclei with evenly stained chromatin (Fig. 2*A*). FISH with chromosome-specific probes indicated that fragmented nuclei contained an increased number of chromosomes, which were unevenly distributed among the micronuclei (Fig. 2*B*). Such nuclear changes are characteristic of mitotic catastrophe (5, 6). The percentage of attached micronucleated cells increased over the time of exposure (Fig. 1*B*). As previously reported for γ-irradiated HT1080 cells (37), doxorubicin treatment produced little evidence of apoptosis, judging by the rarity of cells with apoptotic morphology, terminal deoxynucleotidyl transferase-mediated nick end labeling-positive cells, or cells with elevated annexin levels (data not shown). The only measurable change that is usually associated with apoptosis (but may also reflect the formation of micronuclei; Ref. 6) is the appearance of nuclei with decreased (sub-G_1) DNA content, detected after combining attached and floating cells on each plate (Fig. 1*B*). The removal of drug after 3 days slightly accelerated the process of cell death (Fig. 1*A*) and increased the percentages of micronucleated and sub-G_1 cells (Fig. 1*B*).

Many doxorubicin-treated cells also showed phenotypic changes that resembled features of senescence in normal fibroblasts. This SLP included enlarged and flattened morphology, expression of the senescence marker SA-β-gal detectable by 5-bromo-4-chloro-3-indolyl β-D-galactoside (X-gal) staining at pH 6.0 (Fig. 2c,d) and increased granularity (see below). SA-β-gal expression was observed in only

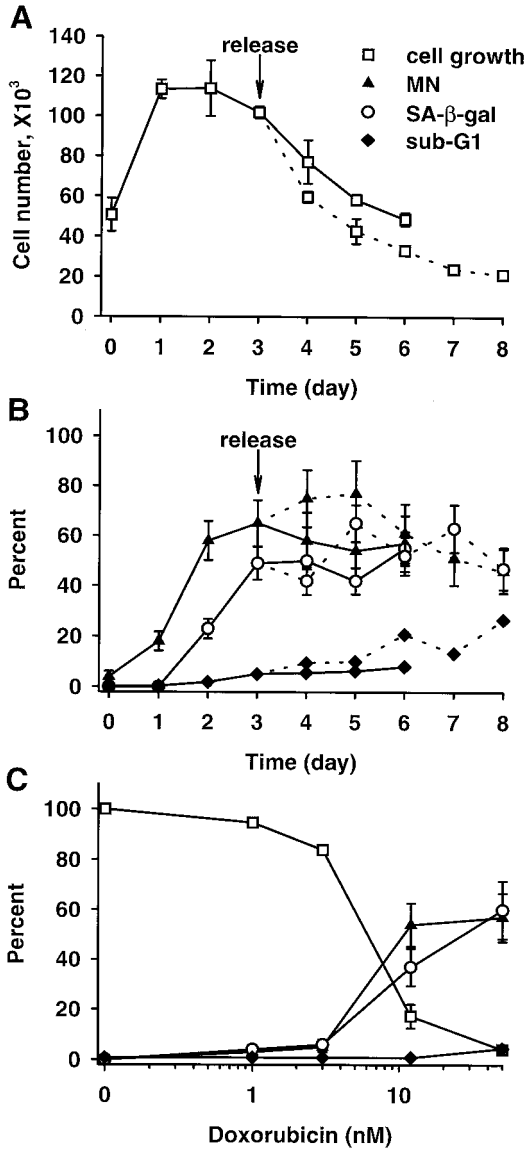

Fig. 1. Effects of doxorubicin on HT1080 3′SS6 cells. *A*, changes in cell number during treatment with 30 nM doxorubicin. Cells were exposed to drug either continuously (*solid lines*) or released from the drug after 3 days of exposure (*dashed lines*). *B*, changes in the percentages of cells with multiple micronuclei (*MN*), SA-β-gal+ cells, and cells with sub-G_1 DNA content during treatment with 30 nM doxorubicin. *Bars*, the Poisson SD calculated as the square root of counted events and expressed as percentages. *C*, growth inhibition (cell number relative to untreated cells) and percentages of cells with multiple micronuclei, SA-β-gal+ cells and cells with sub-G_1 DNA contents, as a function of doxorubicin concentration on 4-day exposure.

[4] B. Schott and I. B. Roninson, unpublished data.

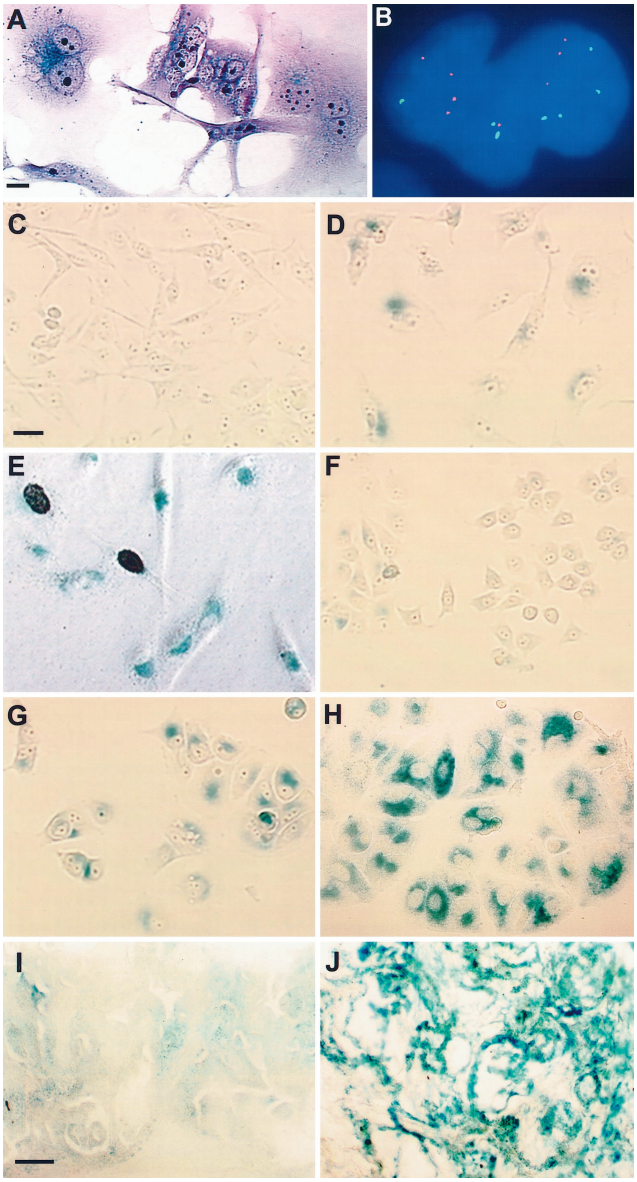

Fig. 2. Formation of micronuclei and SA-β-gal expression in drug-treated cells. Attached cells (*A* and *C-H*) or frozen sections (*I* and *J*) were fixed with 2% formaldehyde/0.2% glutaraldehyde and stained for SA-β-gal activity; cells were counterstained with H&E (*A*) and autoradiographed (*E*). The photographs were taken at 400-fold (*A*; 20-μm scale bar), 1000-fold (*B*), 200-fold (*C-H*; 50-μm scale bar in *C*), or 400-fold (*I* and *J*; 30-μm scale bar in *I*) magnification. *A*, multiple micronuclei in HT1080 (3′SS6) cells treated with 30 nM doxorubicin for 3 days. *B*, FISH analysis of chromosome distribution among the micronuclei in a partially fragmented nucleus of HT1080 cells treated with 20 nM doxorubicin for 3 days. Cells were hybridized with a mixture of fluorescent probes specific for chromosomes 18 (*green*) and 21 (*red*); nuclei were stained with DAPI (*blue*). *C*, untreated HT1080 cells. *D*, HT1080 3′SS6 cells exposed to 30 nM doxorubicin for 4 days. *E*, HT1080 3′SS6 cells treated with 20 nM doxorubicin for 3 days and grown without drug for 4 days, with [^{3}H]thymidine added for the last 2 days. *F*, untreated MCF-7 cells. *G*, MCF-7 cells exposed to 50 nM doxorubicin for 2 days. *H*, MCF-7 cells exposed to 100 nM tRA for 8 days. *I*, xenograft tumor formed by MCF10AneoT cells in nude mice, untreated. *J*, MCF10AneoT xenograft treated *in vivo* with 4-HPR.

1–3% of untreated subconfluent cells, but this percentage rose sharply after 2 days of drug exposure and reached 55% by day 6 (Fig. 1*B*). The removal of doxorubicin on day 3 had no significant effect on the SA-β-gal+ fraction (Fig. 1*B*). On 4-day exposure to different doses of doxorubicin, the percentages of micronucleated and SA-β-gal+ cells showed similar magnitude and drug dose dependence, whereas the sub-G_1 fraction remained low (Fig. 1*C*). The intensity of cellular staining for SA-β-gal also increased in a time- and dose-dependent manner (data not shown). SA-β-gal+ and SA-β-gal− cells underwent mitotic death with a similar probability. For example, cell population treated with 30 nM doxorubicin for 3 days showed micronucleation in 70 ± 8.1% of SA-β-gal+ and 67 ± 8.6% of SA-β-gal− cells; analysis of two other drug-treated populations also showed no significant differences in micronucleation between SA-β-gal+ and SA-β-gal− cells, suggesting that the induction of SLP and mitotic cell death were independent events.

We have also analyzed the response of HT1080 3′SS6 cells to other cytotoxic drugs or ionizing radiation at doses that induced 85% growth inhibition after 4-day continuous exposure (ID_{85}). As summarized in Table 1, all of the agents induced micronucleation in a large fraction (45–66%) of treated cells, whereas the sub-G_1 fraction did not exceed 13% for any of the tested drugs. The increase in the percentage of SA-β-gal+ cells varied for different agents, with the strongest effect (>50%) observed with doxorubicin, aphidicolin, and cisplatin and the weakest effect (<10%) observed with microtubule-affecting agents vincristine and Taxol (Table 1). Induction of reversible growth arrest by serum withdrawal produced faint SA-β-gal staining in some of the cells, but the staining intensity was weaker than in cells treated with any of the drugs. Thus, induction of SLP and mitotic death seem to be common responses of HT1080 cells to different classes of drugs.

SLP Is Associated with Restricted Proliferative Capacity. To investigate whether drug-induced SLP is associated with a restricted proliferative capacity, as would be expected for senescent cells, HT1080 cells were treated with 20 nM doxorubicin for 3 days and then labeled with a lipophilic fluorescent compound, PKH2. PKH2 incorporates stably into plasma membrane and is evenly divided between daughter cells, allowing one to distinguish cells that underwent a different number of divisions by their decreasing PKH2 fluorescence (38). FACS analysis of cells released into drug-free media (Fig. 3*A*) showed that drug-treated cells started dividing on the 1st day after release from the drug, but they divided slower and more heterogeneously than the untreated cells. By day 5 after release from the drug, a shoulder of growth-retarded cells became distinct from the peak of proliferating cells, and PKH2 fluorescence of this shoulder remained almost unchanged on subsequent days (Fig. 3*A*). By day 6, the proliferating cells went through four to five cell divisions, whereas 84% of growth-retarded cells divided only once or twice. Only 8–14% of the growth-retarded cells failed to divide at least once after release from the drug, indicating that growth retardation in this population was not merely a failure to reenter cell cycle after drug-induced growth arrest.

To investigate the association between growth retardation, SLP, and clonogenic potential of drug-treated cells, we have used FACS analysis to separate the growth-retarded and proliferating fractions after drug treatment. We have observed that growth-retarded cells with high PKH2 fluorescence also showed elevated 90-degree light scatter [side scatter (*SS*)] relative to untreated cells (Fig. 3*B*). Elevated side scatter is characteristic of senescent cells and may reflect increased cell size (39) and number of lipofuscin granules (27). Fractions enriched in growth-retarded ($PKH2^{hi}$ SS^{hi}) or proliferating

Table 1 *Effects of different agents on HT1080 3′SS6 cells*

Agent	ID_{85}	% SA-β-gal+	% micronucleated	% sub-G_1
None		1	1.5	0.4
Doxorubicin	30 nM	79	45	10
Aphidicolin	200 ng/ml	64	45	10
Cisplatin	2.2 μM	55	47	9.3
γ-irradiation	1300 rad	36	63	3.2
Cytarabine	1.5 μM	23	64	7.5
Etoposide	900 nM	15	55	7.5
Taxol	5 ng/ml	9.1	66	7.1
Vincristine	1.5 nM	3.1	62	13

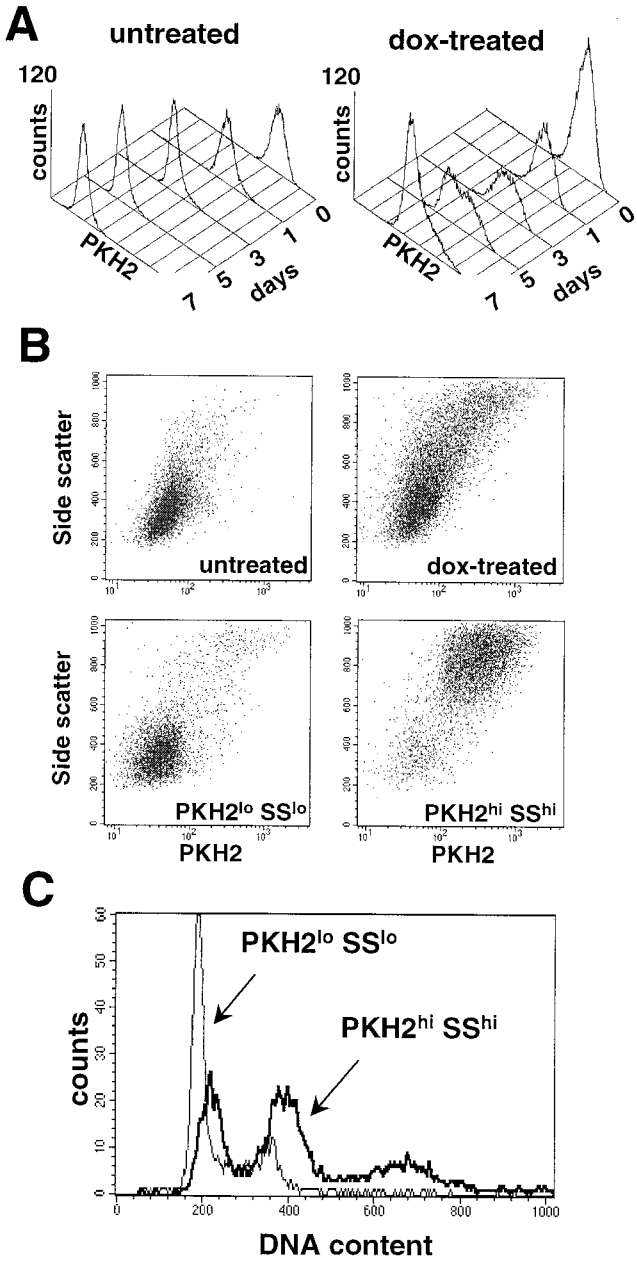

Fig. 3. Flow cytometric analysis of PKH2-labeled HT1080 3′SS6 cells. *A*, changes in PKH2 fluorescence profiles in untreated cells (*left*) and in cells exposed to 20 nM doxorubicin for 3 days, labeled with PKH2, and plated in drug-free medium (*right*). Cells were analyzed by FACS analysis on consecutive days after release from the drug (day 0). For untreated cells, 10,000 PI-negative cells were analyzed on each day. For drug-treated cells, each profile corresponds to the same number of initially plated cells to reflect changes in the cell number. *B*, increased side scatter in growth-retarded cells. Dot density maps of PKH2 fluorescence (*X* axis) and 90-degree light scatter (*Y* axis) are shown for PKH2-labeled untreated cells (*top left*); cells treated for 3 days with 20 nM doxorubicin, labeled with PKH2, and grown without drug for 6 days (*top right*); and for $PKH2^{lo}$ SS^{lo} (*bottom left*) and $PKH2^{hi}$ SS^{hi} (*bottom right*) fractions isolated from the above population by FACS. *C*, DNA content analysis of $PKH2^{lo}$ SS^{lo} (99% pure) and $PKH2^{hi}$ SS^{hi} (95% pure) cell populations isolated by two rounds of FACS sorting after 3 day exposure to 20 nM doxorubicin and 5-day growth without drug.

($PKH2^{lo}$ SS^{lo}) cells were sorted out 5 or 6 days after release from the drug (Fig. 3*B*). The sorted populations were then analyzed for SA-β-gal activity, clonogenicity, and DNA content. The results of three independent sortings are summarized in Table 2. SA-β-gal expression was associated with the growth-retarded fractions, and the percentage of SA-β-gal+ cells in each fraction was close to the percentage of $PKH2^{hi}$ SS^{hi} cells. Colony formation assays showed that $PKH2^{hi}$ SS^{hi} fractions had greatly decreased colony-forming ability relative to $PKH2^{lo}$ SS^{lo} fractions. The residual clonogenicity of growth-retarded fractions correlated with the percentage of $PKH2^{lo}$ SS^{lo} or SA-β-gal− cells in such fractions and was most probably attributable to contamination with proliferating cells (Table 2). Thus, SLP distinguishes cells with restricted proliferative capacity from cells that continue proliferation after release from the drug.

The decreased growth and restricted proliferative capacity of SLP cells were confirmed by other types of assays. For example, we have used [^{3}H]thymidine autoradiography to identify cells that replicated their DNA over a 48-h period starting 3 or 4 days after release from 20 nM doxorubicin (Fig. 2*E*). In two independent experiments, 92–93% of SA-β-gal− cells incorporated [^{3}H]thymidine, but only 28–33% of the SA-β-gal+ population became labeled, indicating that fewer SA-β-gal+ cells underwent DNA replication in the last 2 days before staining. We have also analyzed the long-term proliferation of a largely SLP cell population that survived exposure to a higher drug dose. 10^5 cells were treated with 60 nM doxorubicin for 3 days. Seven days after release from the drug, 15,000 cells remained attached to the plate. Ninety-eight percent of these cells were SA-β-gal+, and ~50% contained micronuclei. Most of these cells eventually died and detached from the plate, but about 1500 SA-β-gal+ single cells or small clusters (<10 cells) remained attached 24 days after release from the drug. Despite periodic renewal of the media, only 25 cell colonies (all SA-β-gal−) grew out by the end of the experiment, indicating that most, if not all, SLP cells lost their long-term proliferative capacity.

Ploidy Changes in SLP Cells. FACS analysis was used to determine the DNA content of $PKH2^{lo}$ SS^{lo} and $PKH2^{hi}$ SS^{hi} fractions isolated 5 days after release from doxorubicin. As shown in Fig. 3*C*, the proliferating ($PKH2^{lo}$ SS^{lo}) fraction showed cell cycle distribution characteristic for exponentially growing cells (high G_1 and S). The growth-retarded ($PKH2^{hi}$ SS^{hi}) fraction showed a heterogeneous DNA content, with broader G_1 and G_2 peaks than in proliferating cells and a substantial fraction of cells with higher than G_2 DNA content. FISH analysis of interphase nuclei confirmed ploidy changes in the growth-retarded cells. Most of the untreated cells were trisomic or near trisomic for chromosomes 13, 18, 21, and X/Y, indicating that the HT1080 3′SS6 line was near-triploid. In contrast, approximately one-half of the cells in the growth-retarded fraction contained enlarged nuclei with four copies of each of the autosomes, whereas ~20% had six or more copies (data not shown). Increased DNA ploidy has been previously associated with terminal stages of senescence in normal fibroblasts (13).

Responses to Doxorubicin in Different Tumor Cell Lines. We have examined cellular changes induced by treatment with moderate doses of doxorubicin in other solid tumor-derived human cell lines. Fourteen lines derived from 10 different types of cancer were treated for 2 days with the doses of doxorubicin that induced 70–90% growth inhibition. The effects of this treatment on the formation of micronuclei, sub-G_1 fraction, and the SA-β-gal+ phenotype are summarized

Table 2 *Analysis of sorted populations of growth-retarded and proliferating fractions of doxorubicin-treated HT1080 cells*[a]

Experiment	Fraction	% $PKH2^{hi}$ SS^{hi}	% SA-β-gal+	No. of colonies/1000 cells
1	GR[b]	82%	64%	26
	P	7%	4.8%	210
2	GR	75%	53%	62
	P	1%	1.2%	254
3	GR	80%	76%	11
	P	1%	3.7%	93

[a] HT1080 (3′SS6) cells were treated with 20 nM doxorubicin for 3 days, labeled with PKH2, and grown without drug for 5 days (experiment 3) or 6 days (experiments 1 and 2).

[b] Growth-retarded (GR) and proliferating (P) cells were isolated by FACS.

Table 3 *Effects of 2-day treatment with moderate doses of doxorubicin in cell lines derived from different types of human solid tumors*

Cell line	Tumor type	Doxorubicin concentration	p53 status[a]	Increased SA-β-gal[b]	Increased micronuclei formation[c]	Increased sub-G_1[d]
HT1080	Fibrosarcoma	20–30 nM	wt[e]	+	+	+
HCT116	Colon carcinoma	50 nM	wt	+	+	++
MCF-7	Breast carcinoma	12–50 nM	wt	+[f]	++	−
HepG2	Hepatocellular carcinoma	250–500 nM	wt	+	++	++
A2780	Ovarian carcinoma	20–50 nM	wt	+[f]	A	+++
LNCaP	Prostate carcinoma	100–500 nM	wt	+[f]	A	+++
HeLa	Cervical carcinoma	400–800 nM	wt/E6	+	++	+
HEp-2	Larynx carcinoma	50–100 nM	wt/E6	+[f]	+	−
DLD1	Colon carcinoma	100–500 nM	mt (241)	−	+	+
SW480	Colon carcinoma	100–150 nM	mt (273)	+	+	−
U251	Glioma	200 nM	mt (273)	+	++	−
MDA-MB-231	Breast carcinoma	50 nM	mt (280)	−	++	−
PC3	Prostate carcinoma	100 nM	mt (del138)	−	+++	++
Saos2[g]	Osteosarcoma	50–60 nM	mt (del)	+	+	++

[a] p53 status of the listed cell lines is from Refs. 48–55.
[b] Positive (*) indicates ≥3-fold increase in the percentage of SA-β-gal+ cells.
[c] Micronucleated cells: +, 20–50%; ++, 50–80%; +++, ≥80%; A, predominance of cells with apoptotic morphology.
[d] Sub-G_1 cells: +, 5–10%; ++, 10–30%; +++, ≥30%.
[e] Wt, wild type; mt, mutant.
[f] More than 10% SA-β-gal+ cells without drug treatment.
[g] Because of long doubling time of Saos2 cells, all the assays were carried out after 4-day exposure to doxorubicin.

in Table 3. Drug treatment increased the fraction of micronucleated cells in almost all of the cell lines, but only two lines (LNCaP and A2780) showed predominant morphological changes characteristic of apoptosis. The same two lines were the only ones to develop a very high (≥48%) sub-G_1 fraction (Table 3), suggesting that mitotic death may be more common than apoptosis among solid tumor cell lines exposed to moderate doses of doxorubicin.

SA-β-gal+ cells with morphological features of senescence were induced by doxorubicin treatment in 11 of 14 lines (Table 3). One of these lines, HCT116 colon carcinoma was analyzed with regard to a correlation between SA-β-gal staining and growth arrest. HCT116 cells were treated with 50 nM doxorubicin for 3 days and stained for SA-β-gal expression 10–11 days after release from the drug. At this point, the proliferating cell colonies were almost entirely SA-β-gal−, whereas attached single cells were mostly SA-β-gal+, indicating that SA-β-gal expression in this cell line was associated primarily with cells that failed to divide even once after release from the drug.

SA-β-gal induction was observed in all eight of the tested lines that carry wild-type p53, including two lines in which the function of p53 is inhibited by the E6 papilloma virus protein. Several cell lines (MCF-7, A2780, LNCaP, and HEp-2) showed noticeable SA-β-gal positivity (>10%) even without drug treatment, but these levels were further increased on exposure to doxorubicin (as illustrated for MCF-7 cells in Fig. 2, *F* and *G*). SA-β-gal expression of untreated cells varied depending on the media and among subclones; it remains to be determined whether the background SA-β-gal activity marks cells that spontaneously lose their proliferative capacity. Doxorubicin also induced SA-β-gal in three of six p53-mutant cell lines, including Saos-2, which is deficient not only for p53 but also for Rb. All three lines that failed to show SA-β-gal induction under the tested conditions were p53-mutant. Thus, induction of the SA-β-gal marker of senescence by drug treatment is common in solid tumor cells and may partly correlate with the p53 status.

Cytostatic Treatment with Retinoids Induces SLP in Breast Carcinoma Cells *in Vitro* and *in Vivo*. Inhibition of tumor cell growth by doxorubicin and other chemotherapeutic drugs depends both on their cytotoxic and cytostatic effects. To determine whether SLP would be induced by agents, the action of which is primarily cytostatic, we have investigated the effect of retinoids that cause differentiation-associated permanent growth arrest in breast carcinoma cells (40). MCF-7 breast carcinoma cells were labeled with PKH2 and grown in the presence or absence of 100 nM tRA. FACS analysis of PKH2 fluorescence indicated that tRA-treated and untreated cells divided at the same rate over the first 4 days, but retinoid-treated cells slowed down their division by day 6, and essentially stopped dividing between days 6 and 9 (Fig. 4*A*). Concurrent determination of the cell number showed that tRA-treated cells started growing slower than untreated cells between days 4 and 6, and showed only a small (20%) decrease in cell number between days 6 and 9 (Fig. 4*B*). These results, together with a small difference in the number of dead (propidium iodide-positive) cells between tRA-treated and untreated samples, indicated that growth inhibition of

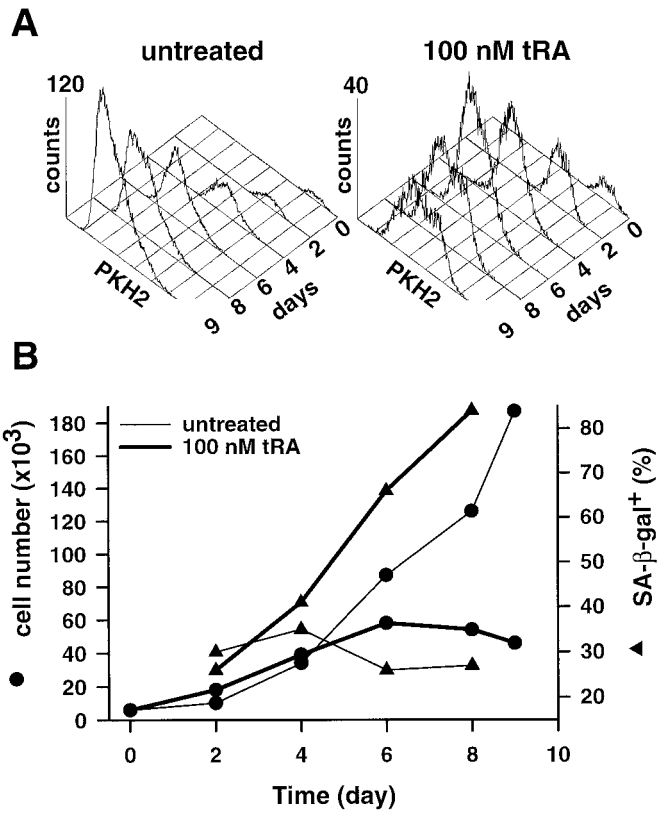

Fig. 4. Effects of tRA on MCF-7 cells *A*, PKH2 profiles of untreated MCF-7 cells and cells treated with 100 nM tRA for the indicated number of days. Each profile corresponds to the same number of initially plated cells. *B*, time course of changes in cell number (●) and percentages of SA-β-gal+ cells (▲) for MCF-7 cells, untreated or treated with 100 nM tRA.

MCF-7 cells by 100 nM tRA was due primarily to the cytostatic effect of this agent. The clonogenicity of cells treated for 9 days with tRA decreased >100-fold relative to untreated cells, indicating permanent nature of this cytostatic growth inhibition.

Retinoid-treated MCF-7 cells showed enlarged and flattened morphology and increased granularity. These changes have been described as characteristic of differentiation in this cell line (12, 41), but can also be viewed as indicative of a senescence-like process. In agreement with this interpretation, tRA treatment drastically increased SA-β-gal expression in MCF-7 cells (Fig. 3, *F* and *H*). The percentage of SA-β-gal+ cells increased in parallel with growth inhibition and reached 84% on day 8 (Fig. 4*B*). Thus, the induction of SLP correlates with retinoid-induced cytostatic growth arrest.

We have also investigated whether SLP could be induced by retinoid treatment *in vivo*. As a model system, we have used H-*ras*-transformed MCF10ANeoT human breast epithelial cell line; when grown as a xenograft in athymic nude mice, this line forms hyperplastic and premalignant lesions with characteristics of ductal hyperplasia and carcinoma *in situ* of human breast (42). Previous *in vitro* studies indicated that 4-HPR, an inhibitor of mammary carcinogenesis, suppresses cell proliferation in MCF10AneoT cells (43). MCF10AneoT cells were transplanted into the mammary gland parenchyma of both inguinal glands of 10 nude mice. After 4–5 weeks, 4–6 mm/diameter tumor nodules occurred in all animals. Two groups, each including five animals (10 tumors), were either untreated or treated with 4-HPR for 2 months at 4 mM/kg diet. Untreated tumors showed three types of glandular structures: simple tubular (20%), hyperplastic tubular (58%), and premalignant with dysplastic epithelial cells (22%). 4-HPR-treated tumors showed an increase in simple tubular structures (55%) and a decrease in tubular hyperplastic (35%) and premalignant structures (10%). These observations suggested that 4-HPR induced differentiation in MCF10ANeoT xenografts. Frozen sections from 4-HPR-treated and untreated tumors were stained for SA-β-gal expression. Both tumors showed detectable SA-β-gal staining in xenograft epithelial cells. In the untreated tumor, the staining was of low intensity and localized to limited tumor areas (Fig. 2*I*), whereas the drug-treated tumor showed higher SA-β-gal staining intensity with relatively uniform distribution among the tumor cells (Fig. 2*J*), suggesting that retinoid treatment *in vivo* induced SLP in tumor cells.

DISCUSSION

Induction of accelerated senescence was proposed to be a programmed protective response of normal cells to potentially carcinogenic impact (21). In this regard, rapid senescence serves a similar function to apoptosis; remarkably, both of these responses to cellular damage are regulated largely by p53. It is well appreciated that the program of apoptosis is retained in many types of leukemias and solid tumors, and that apoptosis contributes to tumor response to anticancer agents. Senescence, however, has been viewed primarily as a property of normal cells, which is lost during neoplastic transformation. The results of the present study indicate that phenotypic and proliferative changes that resemble terminal stages of replicative senescence can be induced in tumor cells not only through genetic modifications but also epigenetically, by treatment with different classes of anticancer agents. Drug-induced SLP distinguishes cells with restricted proliferative potential from those that continue to proliferate after drug exposure, suggesting that senescence-like terminal proliferation arrest is an important determinant of treatment response in human cancer.

Cellular changes that define SLP include enlarged and flattened morphology, increased granularity, expression of SA-β-gal, and ploidy changes. All of these features have been originally associated with terminal stages of replicative senescence in normal fibroblasts (13, 16). There are some obvious differences, however, between the slow process of replicative senescence (about 50 cell doublings) and the more rapid forms of terminal proliferation arrest, activated in normal or tumor cells in response to different stimuli. Most significantly, replicative senescence is mediated, at least in part, by the shortening of telomeres (25), but there is no apparent decrease in telomerase activity in drug-treated HT1080 cells (44), in nasopharyngeal carcinoma cells that display SLP after cisplatin treatment (31), or in tumor cells that are growth-arrested by overexpression of p53 (28). Telomere shortening during senescence was suggested to trigger terminal proliferation arrest through p53 activation (45). p53 also plays a key role in senescence-like terminal proliferation arrest induced by DNA damage or *ras* mutation in normal cells (18, 20). In the present study, all three cell lines that failed to induce SLP after treatment with moderate doses of doxorubicin were p53-deficient, whereas this response was observed in all cell lines with wild-type p53. As will be reported elsewhere (46), p53 acts as a positive regulator of drug-induced SLP in HT1080 and HCT116 cell lines, although its function is not absolutely required for this drug response. These observations suggest that various physiological and damage-induced stimuli may activate the same senescence-like response in normal and tumor cells and that SLP marks this common program of terminal proliferation arrest.

In cells treated with cytotoxic drugs, SLP induction and cell death seem to be concurrent and independent responses. Thus, SA-β-gal+ and SA-β-gal− cells have a similar probability of undergoing mitotic death during drug treatment or on the first few days after release from the drug. Once the rapid process of cell death is completed, however, SLP distinguishes the subpopulation of growth-retarded and nonclonogenic cells from the cells that recover and proliferate normally. The overall outcome of treatment with chemotherapeutic drugs is, therefore, determined by the combination of factors responsible for the induction of cell death (mitotic death or apoptosis) and senescence-like terminal proliferation arrest. Exposure to moderate doses of doxorubicin induced SLP in 11 of 14 tested cell lines derived from different types of human solid tumors. Among the different effects of doxorubicin in this panel of tumor cell lines, mitotic cell death and SLP seem to be more common than apoptosis. SLP is relatively more prominent at less cytotoxic drug doses (such as 20–100 nM doxorubicin), which can be readily induced and maintained for a long period of time in patients' plasma by continuous infusion (47). Senescence-like terminal proliferation arrest may, therefore, be a significant determinant of tumor response to continuous infusion protocols. On the other hand, SLP correlates with permanent growth inhibition of breast carcinoma cells by retinoids, under the conditions in which the induction of cell death plays a minimal role in their antiproliferative effect. Thus, SLP induction may be the primary determinant of treatment outcome for cytostatic differentiating agents.

Analysis of SLP markers in clinical cancer may provide an important diagnostic approach to monitoring tumor response to different forms of therapy. SA-β-gal expression is thus far the only quantifiable marker associated with drug-induced SLP *in vitro* and *in vivo*. In the present study, drug-induced SA-β-gal expression was found to correlate with terminal proliferation arrest in all three cell lines (HT1080, MCF7, and HCT116) in which such correlation was investigated. On the other hand, the sensitivity of the SA-β-gal assay, the background SA-β-gal levels in untreated cells, and the timing of SA-β-gal expression relative to growth arrest varied for different lines. Identification of more general and specific SLP markers should be useful for future studies on clinical tumor samples. SLP induction may also provide the basis for a screening assay for agents that would enhance terminal proliferation arrest induced by differentiating agents or low doses of cytotoxic drugs. Elucidation of the molecular determinants of senescence-like terminal proliferation arrest should suggest approaches to augmenting this desirable response and thereby increasing the efficacy of cancer treatment.

ACKNOWLEDGMENTS

We thank Dr. B. Vogelstein for HCT116 cells; Dr. F. R. Miller for MCF10AneoT cells; Drs. M. Polonskaia, K. Hagen, and J. Schnell for assistance with flow sorting; M. Chmyra and Dr. Y. Verlinsky for FISH assays; Dr. S. Salov for help with cell line maintenance; and Dr. A. V. Gudkov for helpful discussions.

REFERENCES

1. Hickman, J. A. Apoptosis induced by anticancer drugs. Cancer Metastasis Rev., *11:* 121–139, 1992.
2. Lowe, S. W., Ruley, H. E., Jacks, T., and Housman, D. E. p53-dependent apoptosis modulates the cytotoxicity of anticancer agents. Cell, *74:* 957–968, 1993.
3. Hendry, J. H., and West, C. M. L. Apoptosis and mitotic cell death: their relative contributions to normal-tissue and tumor radiation response. Int. J. Radiat. Biol., *71:* 709–719, 1997.
4. Tounekti, O., Pron, G., Belehradek, J., Jr., and Mir, L. M. Bleomycin, an apoptosis-mimetic drug that induces two types of cell death depending on the number of molecules internalized. Cancer Res., *53:* 5462–5469, 1993.
5. Lock, R. B., and Stribinskiene, L. Dual modes of death induced by etoposide in human epithelial tumor cells allow Bcl-2 to inhibit apoptosis without affecting clonogenic survival. Cancer Res., *56:* 4006–4012, 1996.
6. Torres, K., and Horwitz, S. B. Mechanisms of Taxol-induced cell death are concentration-dependent. Cancer Res., *58:* 3620–3626, 1998.
7. Demarcq, C., Bunch, R. T., Creswell, D., and Eastman, A. The role of cell cycle progression in cisplatin-induced apoptosis in Chinese hamster ovary cells. Cell Growth Differ., *5:* 983–993, 1994.
8. Merritt, A. J., Allen, T. D., Potten, C. S., and Hickman, J. A. Apoptosis in small intestinal epithelia from p53-null mice: evidence for a delayed, p53-independent G_2-M-associated cell death after γ-irradiation. Oncogene, *14:* 2759–2766, 1997.
9. Waldman, T., Lengauer, C., Kinzler, K. W., and Vogelstein, B. Uncoupling of S phase and mitosis induced by anticancer agents in cells lacking p21. Nature (Lond.), *381:* 713–716, 1996.
10. Bunz, F., Dutriaux, A., Lengauer, C., Waldman, T., Zhou, S., Brown, J. P., Sedivy, J. M. Kinzler, K. W., and Volgelstein, B. Requirement for p53 and p21 to sustain G_2 arrest after DNA damage. Science (Washington DC), *282:* 1497–1501, 1998.
11. Kung, A. L., Zetterberg, A., Sherwood, S. W., and Schimke, R. T. Cytotoxic effects of cell cycle phase specific agents: results of cell cycle perturbation. Cancer Res., *50:* 7307–7317, 1990.
12. Fornari, F. A. Jr., Jarvis, W. D., Grant, S., Orr, M. S., Randolph, J. K., White, F. K. H., Mumaw, V. R., Lovings, E. T., Freeman, R. H., and Gewirtz, D. A. Induction of differentiation and growth arrest associated with nascent (nonoligosomal) DNA fragmentation and reduced *c-myc* expression in MCF-7 human breast tumor cells after continuous exposure to a sublethal concentration of doxorubicin. Cell Growth Differ., *5:* 723–733,1994.
13. Hayflick, L., and Moorhead, P. S. The serial cultivation of human diploid cell strains. Exp. Cell Res., *37:* 585–621, 1961.
14. Smith, J. R., and Pereira-Smith, O. M. Replicative senescence: implications for *in vivo* aging and tumor suppression. Science (Washington DC), *273:* 63–67, 1996.
15. Duncan, E. L., and Reddel, R. R. Genetic changes associated with immortalization. Biochemistry, *62:* 1263–1274, 1997.
16. Dimri, G. P., Xinhua, L., Basile, G., Acosta, M., Scott, G., Roskelley, C., Medrano, E. E., Linskens, M., Rubej, I., Pereira-Smith, O., Peacocke, M., and Campisi, J. A biomarker that identifies senescent human cells in culture and in aging skin *in vivo*. Proc. Natl. Acad. Sci. USA, *92:* 9363–9367, 1995.
17. Chen, Q., and Ames, B. N. Senescence-like growth arrest induced by hydrogen peroxide in human diploid fibroblast F65 cells. Proc. Natl. Acad. Sci. USA, *91:* 4130–4134, 1994.
18. DiLeonardo, A., Linke, S. P., Clarkin, K., and Wahl, G. M. DNA damage triggers a prolonged p53-dependent G_1 arrest and long-term induction of Cip1 in normal human fibroblasts. Genes Dev., *8:* 2540–2551, 1994.
19. Robles, S. J., and Adami, G. R. Agents that cause DNA double strand breaks lead to $p16^{INK4A}$ enrichment and the premature senescence of normal fibroblasts. Oncogene, *16:* 1113–1123, 1998.
20. Serrano, M., Lin, A. W., McCurrach, M. E., Beach, D., and Lowe, S. W. Oncogenic ras provokes premature cell senescence associated with accumulation of p53 and p16INK4a. Cell, *88:* 593–602, 1997.
21. Weinberg, R. A. The cat and mouse games that genes, viruses and cells play. Cell, *88:* 573–575, 1997.
22. Ko, L. J., and Prives, C. p53: puzzle and paradigm. Genes Dev., *10:* 1054–1072, 1996.
23. Linke, S. P., Clarkin, K. C., and Wahl, G. M. p53 mediates permanent arrest over multiple cell cycles in response to γ-irradiation. Cancer Res., *57:* 1171–1179, 1997.
24. Whitaker, N. J., Bryan, T. M., Bonnefin, P., Chang, A. C-M., Musgrove, E. A., Breithwaite, A. W., and Reddel, R. R. Involvement of RB-1, p53, $p16^{INK4}$ and telomerase in immortalization of human cells. Oncogene, *11:* 971–976, 1995.
25. Shay, J. W. Telomerase in human development and cancer. J. Cell Physiol., *173:* 266–270, 1997.
26. Pereira-Smith, O. M., and Smith, J. R. Genetic analysis of indefinite division in human cells: identification of four complementation groups. Proc. Natl. Acad. Sci. USA, *85:* 6042–6046, 1988.
27. Sugrue, M. M., Shin, D. Y., Lee, S. W., and Aaronson, S. A. Wild-type p53 triggers a rapid senescence program in human tumor cells lacking functional p53. Proc. Natl. Acad. Sci. USA, *94:* 9648–9653, 1997.
28. Xu, H-J., Zhou, Y., Ji, W., Perng, G-S., Kruzelock, R., Kong, C-T., Bast, R. C., Mills, G. B., Li, J., and Hu, S-X. Reexpression of the retinoblastoma protein in tumor cells induces senescence and telomerase inhibition. Oncogene, *15:* 2589–2596, 1997.
29. Uhrbom, L., Nister, M., and Westermark, B. Induction of senescence in human malignant glioma cells by $p16^{INK4A}$. Oncogene, *15:* 505–514, 1997.
30. Vogt, M., Haggblom, C., Yeargin, J., Christiansen-Weber, T., and Haas, M. Independent induction of senescence by $p16^{INK4a}$ and $p21^{CIP1}$ in spontaneously immortalized human fibroblasts. Cell Growth Differ., *9:* 139–146, 1998.
31. Wang, X., Wong, S. C., Pan, J., Tsao, S. W., Fung, K. H., Kwong, D. L., Sham, J. S., Nicholls, J. M. Evidence of cisplatin-induced senescent-like growth arrest in nasopharyngeal carcinoma cells. Cancer Res., *58:* 5019–5022, 1998.
32. Chang, B-D., and Roninson, I. B. Inducible retroviral vectors regulated by *lac* repressor in mammalian cells. Gene, *183:* 137–142, 1996.
33. Perry, M. E., Rolfe, M., McIntyre, P., Commane, M., and Stark, G. R. Induction of gene amplification by 5-aza-2′-deoxycytidine. Mutat. Res., *276:* 189–197, 1992.
34. Jordan, M. A., Wendell, K., Gardiner, S., Derry, W. B., Copp, H., and Wilson, L. Mitotic block induced in HeLa cells by low concentrations of paclitaxel (Taxol) results in abnormal mitotic exit and apoptotic cell death. Cancer Res., *56:* 816–825, 1996.
35. Brown, R., Marshall, C. J., Pennie, S. G., and Hall, A. Mechanism of activation of an N-*ras* gene in the human fibrosarcoma cell line HT1080. EMBO J., *3:* 1321–1326, 1984.
36. Li, W., Fan, J., Hochhauser, D., Banerjee, D., Zielinski, Z., Almasan, A., Yin, Y., Kelly, R., Wahl, G. M., and Bertino, J. R. Lack of functional retinoblastoma protein mediates increased resistance to antimetabolites in human sarcoma cell lines. Proc. Natl. Acad. Sci. USA, *24:* 10436–10440, 1995.
37. Pellegata, N. S., Antoniono, R. J., Redpath, J. L., and Stanbridge, E. J. DNA damage and p53-mediated cell cycle arrest: a reevaluation. Proc. Natl. Acad. Sci. USA, *93:* 15209–15214, 1996.
38. Horan, P. K., and Slezak, S. E. Stable cell membrane labeling. Nature (Lond.), *340:* 167–168, 1989.
39. Sherwood, S. W., Rush, D., Ellsworth, J. L., and Schimke, R. T. Defining cellular senescence in IMR-90 cells: a flow cytometric analysis. Proc. Natl. Acad. Sci. USA, *85:* 9086–9090, 1988.
40. Ueda, H., Takenawa, T., Millan, J. C., Gesell, M. S., and Brandes, D. The effects of retinoids on proliferative capacities and macromolecular synthesis in human breast cancer MCF-7 cells. Cancer (Phila.), *15:* 2203–2209, 1980.
41. Guilbaud, N. F., Gas, N., Dupont, M. A., and Valette, A. Effects of differentiation-inducing agents on maturation of human MCF-7 breast cancer cells. J. Cell Physiol., *145:* 162–172, 1990.
42. Miller, F. R., Soule, H. D., Tait, L., Pauley, R. J., Wolman, S. R., Dawson, P. J., and Heppner, G. H. Xenograft model of progressive human proliferative breast disease. J. Natl. Cancer Inst., *85:* 1725–1732, 1993.
43. Moon, R. C., Mehta, R. G., and Rao, K. V. N. Retinoids and cancer in experimental animals. *In:* M. B. Sporn, A. B. Roberts, and D. S. Goodman (eds.), The Retinoids, Biology, Chemistry, and Medicine, pp. 573–595. New York: Raven Press, 1994.
44. Holt, S. E., Aisner, D. L., Shay, J. W., and Wright, W. E. Lack of cell cycle regulation of telomerase activity in human cells. Proc. Natl. Acad. Sci. USA, *94:* 10687–10692, 1997.
45. Vaziri, H., West, M. D., Allsopp, R. C., Davison, T. S., Wu, Y. S., Arrowsmith, C. H., Poirier, G. G., and Benchimol, S. ATM-dependent telomere loss in aging human diploid fibroblasts and DNA damage lead to the post-translational activation of p53 protein involving poly(ADP-ribose) polymerase. EMBO J., *16:* 6018–6033, 1997.
46. Chang, B. D., Xuan, Y., Broude, E. V., Zhu, H., Schott, B., Fang, J., and Roninson, I. B. Role of p53 and $p21^{waf1/cip1}$ in senescence-like terminal proliferation arrest induced in human tumor cells by chemotherapeutic drugs. Oncogene, 1999, in press.
47. Speth, P. A., Linssen, P. C., Boezeman, J. B., Wessels, H. M., and Haanen, C. Cellular and plasma adriamycin concentrations in long-term infusion therapy of leukemia patients. Cancer Chemother. Pharmacol., *20:* 305–310, 1987.
48. Debernardis, D., Sire, E. G., DeFeudis, P., Vikhanskaya, F., Valenti, M., Russo, P., Parodi, S., D'Incalci, M., and Broggini, M. p53 status does not affect sensitivity of human ovarian cancer cell lines to paclitaxel. Cancer Res., *57:* 870–874, 1997.
49. Diller, L., Kassel, J., Nelson, C. E., Gryka, M. A., Litwak, G., Gebbardt, M., Bressac, B. Ozturk, M., Baker, S. J., Vogelstein, B., and Friend, S. H. p53 functions as a cell cycle control protein in osteosarcomas. Mol. Cell. Biol., *10:* 5772–5781, 1990.
50. Hosono, S., Lee, C. S., Chou, M. J., Yang, C. S., and Shih, C. H. Molecular analysis of the *p53* alleles in primary hepatocellular carcinomas and cell lines. Oncogene, *6:* 237–243 1991.
51. Kim, M. S., Li, S. L., Bertolami, C. N., Cherrick, H. M., and Park, N. H. State of p53, Rb and DCC tumor suppressor genes in human oral cancer cell lines. Anticancer Res., *13:* 1405–1413, 1993.
52. O'Connor, P. M., Jackman, J., Bae, I., Myers, T. G., Fan, S. Mutoh, M., Scudiero, D. A., Monks, A., Sausville, E. A., Weinstein, J. N., Friend, S., Fornace, A. J., Jr., and Kohn, K. W. Characterization of the p53 tumor suppressor pathway in cell lines of the National Cancer Institute anticancer drug screen and correlations with the growth-inhibitory potency of 123 anticancer agents. Cancer Res., *57:* 4285–4300, 1997.
53. Rodrigues, N. R., Rowan, A., Smith, M. E. F., Kerr, I. B., Bodmer, W. F., Gannon, J. V., and Lane, D. P. p53 mutations in colorectal cancer. Proc. Natl. Acad. Sci. USA, *87:* 7555–7559, 1990.
54. Scheffner, M., Munger, K., Byrne, J. C., and Howley, P. M. The state of p53 and retinoblastoma genes in human cervical carcinoma cell line. Proc. Natl. Acad. Sci. USA, *88:* 5523–5527, 1991.
55. Yaginuma, Y., and Westphal, H. Analysis of the *p53* gene in human uterine carcinoma cell lines. Cancer Res., *51:* 6506–6509, 1991.